An Efficient Method to Determine Strain Profiles on FBGs by Using Differential Evolution and GPU

Lucas Hermann Negri, Heitor Silvério Lopes,
Marcia Muller and José Luís Fabris
Graduate Program in Electrical and Computer Engineering
Federal University of Technology - Paraná
Curitiba, Brazil 80230-901
Email: fabris@utfpr.edu.br

Aleksander Sade Paterno
Department of Electrical Engineering
Santa Catarina State University
Joinville, Brazil 89219-710

***Abstract*—This paper shows the application of the Differential Evolution algorithm to the recovery of the deformation profile applied to a fiber Bragg grating sensor (FBG). The method uses only the sensor reflectivity, without the need of phase information, and has been shown to be highly parallelizable. The method was specially implemented to run the complex computations required by the fitness function using a Graphical Processing Unit (GPU). This provided an enhancement of 3 orders of magnitude in the computation time when compared to similar methods shown in literature. Three experiments were performed to evaluate the computational performance of the DE algorithm, and its convergence of the solution to the target deformation profile. Overall, the method is very promising and it can be applied to problems that require a fast response, such as the online monitoring of FBG sensors.**

I. Introduction

A fiber Bragg grating (FBG) is a device produced in the core of an optical fiber that reflects light at a particular wavelength band. FBGs are widely known and used in sensing applications due to its immunity to external electromagnetic fields, natural wavelength multiplexing capabilities, convenience for transmitting data over long distances and high sensitivity to mechanical deformations and temperature changes.

FBG sensors are interrogated by illuminating them with a broadband light source and detecting the spectral position of the reflected band which is related to the measurand. Changes in the measurand are then determined by traditional methods [1] used to detect spectral shifts in the central wavelength of the reflected band. These methods are highly efficient when the external parameters affects uniformly the whole device. Nevertheless, such methods are useless when the FBG sensor is subjected to non uniform perturbations along its length. To solve this drawback, some methods were already proposed in the literature. However, all they have own advantages and limitations, such as requiring the use of phase information of the signal [2]–[6] and using two sensors simultaneously while having a processing time in the order of hours [7].

To circumvent these issues, a method based on the Differential Evolution (DE) algorithm [8], [9] was proposed by Negri et al [10], enabling the recovery of the mechanical deformation profile applied to the FBG. For its application, the method requires only information about the magnitude of the band reflected by the FBG sensor. Although this method has reduced the processing time from hours to tens of seconds, its processing time remained the limitation for applications that require higher acquisition rates or that is aimed at continuous monitoring of the FBG sensor.

This paper proposes important improvements to the DE method previously developed. To take the advantage of the parallel processing capabilities commonly found in Graphical Processing Units (GPUs), the DE method was re-implemented as a parallel procedure. When compared to the earlier method, a significant reduction in the processing time (from tens of seconds to tenths of seconds) was observed.

II. Methodology

The DE algorithm is used to determine mechanical deformation profile applied to an FBG sensor. The profile determination is performed by using the magnitude of the FBG reflection spectrum that can be easily obtained with interrogation methods [1]. This experimentally obtained light spectrum (magnitude only, no phase information) is referenced here as *target spectrum*, and contains enough information about the perturbation in the sensor structure.

The proposed method maintains a population of candidate solutions, where each individual of this population corresponds to one deformation profile. This population is iteratively improved by using DE until a suitable deformation profile is found, whose reflection spectrum matches the target spectrum. This evolutionary process is guided by the fitness evaluation of each individual, that is computed as the error between the target spectrum and the one simulated from the candidate solution. The transfer matrix method was used to simulate the reflection spectrum of each individual.

Among the steps of the proposed evolutionary process, the fitness evaluation is the one which takes more time due to the computational cost of the transfer matrix method. Computing the reflectance of an FBG from its parameters by using the transfer matrix method requires, for each evaluated wavelength, a series of matrix multiplications and, eventually, solving algebraic equations to produce the simulation parameters. To reduce the required computation time, a GPU with capacity of running multiple parallel processes was employed. In this way, fitness evaluation of each individual can occur in parallel taking advantage of the easy parallelization feature of the DE method. Further, the reflectance spectrum computed

978-1-4673-8418-6/15/$31.00 ©2015 IEEE

with the transfer matrix can be itself parallelized, as the computations for each evaluated wavelength is independent and can occur simultaneously, allowing for a finer granularity in the parallelization.

A. Transfer Matrix Method

A way to compute the reflection spectrum of a FBG is by using the matrix transfer method. Starting from the structural information of a FBG, the transfer matrix method allows the analysis of the propagation of electromagnetic waves for a given wavelength in the grating, resulting in the relation between the incident and the reflected power by the FBG. This relationship can be represented by a 2×2 matrix.

For the FBG section under analysis, l is considered as the section length and $\overline{n}$ the mean value of the core refractive index. The modulation Δn_0 of the core refractive index is assumed sinusoidal with period (pitch) Λ (in nm). Therefore, the transfer matrix corresponding to the analyzed section is given by Equation 1, that describes the relationship between the propagating and counter propagating modes at the extremities of the section [11]:

$$\begin{bmatrix} a(0) \\ b(0) \end{bmatrix} = \begin{bmatrix} T_{11} & T_{12} \\ T_{21} & T_{22} \end{bmatrix} \begin{bmatrix} a(l) \\ b(l) \end{bmatrix}, \quad (1)$$

where T_{11} and T_{22} are given by Equation 2, T_{12} and T_{21} are given by Equation 3, $k = \pi \Delta n_0 / \lambda$, $s = (|k|^2 - \Delta\beta^2)^{1/2}$ and $\Delta\beta = 2\overline{n}\pi/\lambda - \pi/\lambda$, where λ is the free-space wavelength (in nm) [11].

$$T_{11} = T_{22}* = \frac{\Delta\beta \sinh(sl) + is\cosh(sl)}{is} \exp(-i\beta_0 l) \quad (2)$$

$$T_{12} = T_{21}* = \frac{k \sinh(sl)}{is} \exp(i\beta_0 l) \quad (3)$$

A schematic representation of an FBG section is shown in Figure 1, where $b(0)$ is the input signal, $b(l)$ is the transmitted signal, $a(0)$ is the reflected signal, and $a(l)$ is the input signal from the other extremity of the fiber. The values of $a(0)$ and $b(0)$ can be computed by using Equation 1, by assuming $a(l) = 0$ and $b(l) = 1$ (arbitrary, non-null value). The reflectance R can be computed from $a(0)$ and $b(0)$ by using Equation 4:

$$R = \left| \frac{a(0)}{b(0)} \right|^2. \quad (4)$$

A FBG subject to a deformation gradient will have its structure changed according to the deformation. Structural changes are associated with the photoelastic effect [11] and the longitudinal dilation which modifies the fiber refractive index and the grating periodicity. If the deformation is uniform along the grating length, the reflected spectrum will be simply the wavelength shifted. Nevertheless, if the deformation has a non uniform profile, the FBG reflected spectrum is dependent on the force distribution along the grating length.

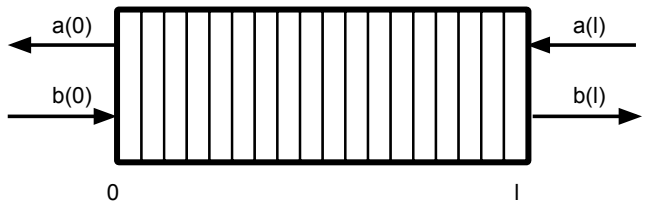

Fig. 1. Schematic representation of an FBG, where the $a(0)$ and $a(l)$ signals are related to the counter-propagating mode, and $b(0)$ and $b(l)$ to the propagating mode.

Gratings with non-uniform structures (apodized or chirped) or subjected to non-uniform deformations profiles can also be modeled by the transfer matrix method by considering the grating as composed of a series of uniform gratings [11]. These uniform gratings can be individually analyzed and the overall FBG response can be obtained by multiplying the resulting transfer matrices. Here, the non uniform FBGs were decomposed in 20 uniform sections as a compromise between accuracy and computational performance. Each section is a FBG with its own structural parameters and subject to an uniform strain ϵ and the new Λ' is then given by Equation 5 and the new mean refractive index value $\overline{n}'$ is given by Equation 6, where p_{11} and p_{12} are the respective photoelastic tensor coefficients of the optical fiber, and ν is the Poisson coefficient.

$$\Lambda' = \Lambda + \Lambda\epsilon \quad (5)$$

$$\overline{n}' = \overline{n} - 0.5\overline{n}^3(p_{12} - \nu(p_{11} + p_{12}))\epsilon. \quad (6)$$

For chirped FBG presenting a linear chirp, Equation 7 can be used to calculate the value of Λ as function of the position z and pitch factor $\delta\Lambda$. For apodized FBG with Gaussian apodization profile, Equation 8 can be used to determine the amplitude of the refractive index modulation envelope in function of the control parameter α, where n_{oc} is the maximum amplitude corresponding to the central point of the Gaussian envelope.

$$\Lambda(z) = \Lambda_0 + (\delta\Lambda/\Lambda_0)z \quad (7)$$

$$\Delta n_0(z) = \Delta n_{oc} \exp\left[-\alpha\left(\frac{z - l/2}{l}\right)^2\right] \quad (8)$$

Figure 2 shows examples of reflection spectra for FBG that are not subject to mechanical deformations, computed by using the transfer matrix method with $l = 1$ cm, $\Lambda = 517$ nm, $\overline{n} = 1.5$ e $\Delta n = 2.5 \times 10^{-4}$, showing the differences in the resulting spectra caused by apodization (a) and chirp (b).

Considering a FBG without chirp, subject to a given deformation profile along its length, if the deformation profile is mirrored along the grating length axis, the magnitude of the spectral response will also be mirrored around the wavelength axis [7], [11]. This mirroring can be verified by the transfer

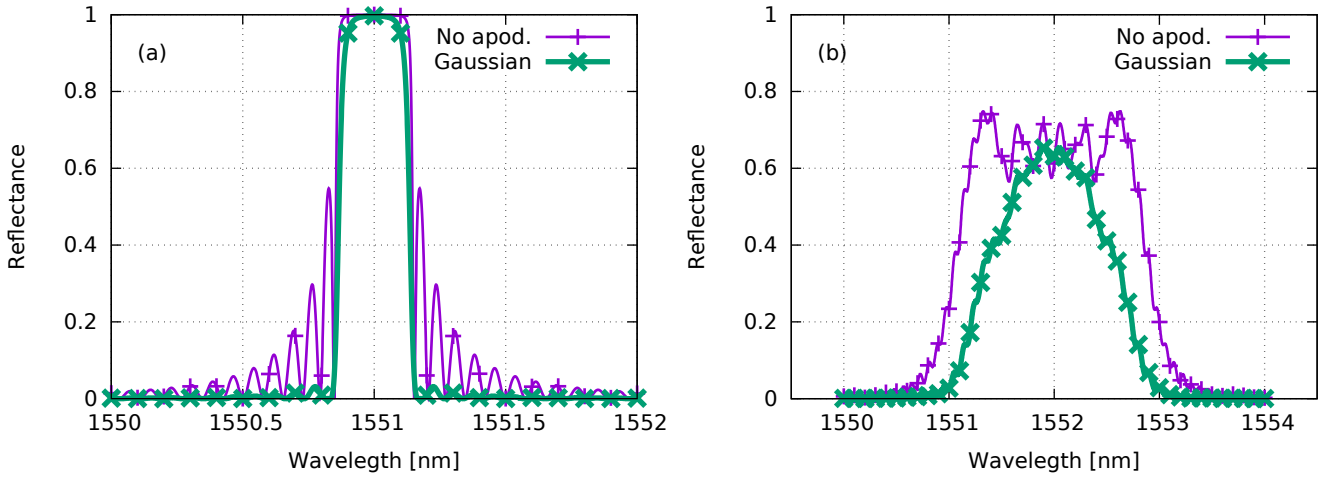

Fig. 2. Examples of FBG reflection spectra simulated by the transfer matrix method, for gratings with $l = 1$ cm, $\Lambda = 517$ nm, $\overline{n} = 1.5$ e $\Delta n = 2.5 \times 10^{-4}$. (a) Spectrum for gratings with uniform Λ, without index apodization and with Gaussian apodization ($\alpha = 5$). (b) Spectrum for gratings with chirp ($\delta\Lambda = 0.65$ nm/cm), without apodization and with Gaussian apodization ($\alpha = 5$).

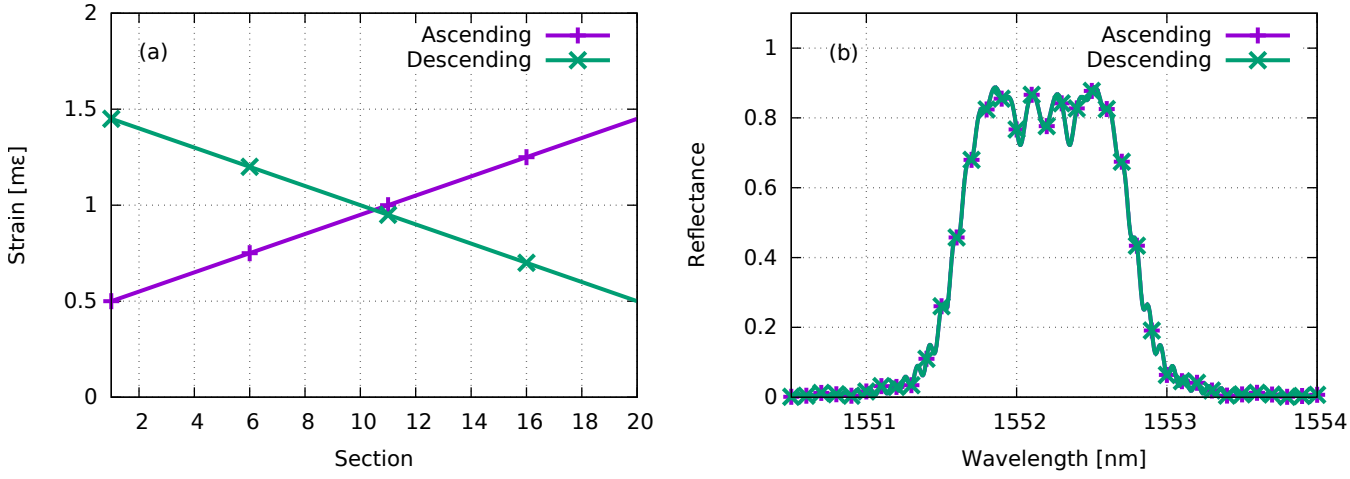

Fig. 3. Two distinct strain profiles applied to the same FBG, resulting in the same reflected signals, in magnitude. (a) Strain profiles. (b) Reflected signals.

matrix method, showing that a FBG with a symmetrical reflection spectrum is insensitive to the mirroring of the deformation profile. This implies that distinct deformation applied to the same FBG will result in the same reflection spectrum if no phase information is available. An example is shown in Figure 3, where two deformation profiles are applied to the same uniform FBG, resulting in similar magnitude responses.

B. Differential Evolution

The DE algorithm was first proposed by [8] and soon gained wide acceptance in the scientific community due to its simplicity and efficiency. Since then, DE has been used successfully in many engineering optimization problems [12], [13]. In this work, for the application of the DE algorithm, a population of 96 individuals (also called vectors) is maintained. Each individual represents a single deformation profile discretized in 20 points. Initially, all individuals are created by a pseudo-random number generator, and then they are iteratively enhanced by the evolution process.

At each iteration of the method, a new trial population is built. Each new individual of the trial population is generated by using an individual from the current population as base, which is modified by means of the crossover and mutation operators. The new individuals are evaluated by the fitness function that measures the similarity between the target spectrum and the spectrum simulated from the individual. These new individuals from the trial population substitute those that served as base for them if the trial individual presents a better fitness evaluation than the current individual. This iterative process continues for $2,000$ iterations, when the individual with the highest fitness value is chosen as the outcome of the method. An overview of the DE algorithm is shown in the fluxogram of Figure 4.

In more details, a DE/rand/1/bin [9] scheme was employed, with a crossover rate $CR = 0.95$ and mutation factor $F = 0.7$. To construct the trial population, the mutation and crossover operators are applied to each individual in the base population (referenced here as *base-individual*). For each base-individual, the mutation operator chooses another three distinct individuals

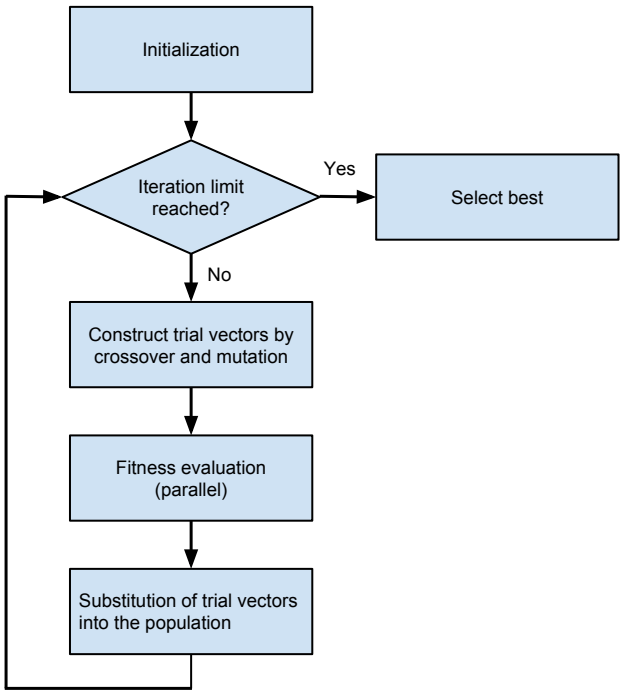

Fig. 4. Flowchart representing the main operations in the differential evolution method employed in this paper.

from the base population and combines them, generating a new mutant individual. With the crossover operator, this mutant individual is recombined with the base-individual, generating a new individual in the trial population. This trial population is evaluated and the individuals from this population take the place of the respective base-individual if there is an improvement in the individual's fitnesses.

The evaluation of an individual consists in simulating the reflection spectrum of the analyzed FBG assuming the application of the the deformation profile represented by the individual. The Mean Squared Error (MSE) between the simulated reflectance and the target spectrum is computed, where the fitness value is inversely proportional to the MSE. Hence, the algorithm searches for a deformation profile that minimizes the MSE.

As shown in Section II-A, distinct deformation profiles can result in a similar reflectance. This ambiguity can be solved by using a FBG with linear chirp, assuring that the situation seen in Figure 3 does not occur, since the FBG reflection spectrum will not be symmetrical anymore. Assuming that there are no abrupt changes in the deformation profile, a smoothness restriction can be added to force the convergence to smooth solutions. Here, a penalty was added to the solutions when a section showed a strain differing more than 0.2 mϵ from the strain in the previous section (in an arbitrary orientation). This penalty was added to the fitness evaluation of the individuals, where the excess difference (excess from the 0.2 mϵ tolerance) between the strain of each section was multiplied by 10 and divided by the total number of sections. The tolerance and weight were chosen arbitrarily and can be changed according to the desired application.

C. Parallel Computation using GPU

In the proposed method, the evaluation of the candidate solutions (individuals) is the most expensive procedure. To evaluate an individual, its reflection spectrum for a given wavelength band must be computed. Each wavelength requires the calculation of the respective transfer matrices, that are then multiplied to compose the grating response. The fitness evaluation of an individual is performed in multiple parallel processes, as the computation of the reflectance at each wavelength is an independent task. The difference between the resulting reflectance and the target spectrum is computed point by point by each process / wavelength, and the total error for an individual is computed by using a parallel *reduce* operator. This possibility of dividing the fitness evaluation in parallel tasks shows that the method can take advantage of a hardware capable of executing parallel processes.

Modern GPUs are developed for the execution of parallel tasks, having multiple parallel processing cores and performing the Single Instruction on Multiple Data (SIMD) points simultaneously. This capabilities makes GPU very suitable for the problem in hand. The CUDA®(Compute Unified Device Architecture) platform was used in this work with a compatible GPU board. Here, the different steps of the DE method were implemented serially for execution on a CPU, with the exception of the fitness evaluation step which was implemented as a *kernel* for parallel execution in a GPU.

The fitness evaluation kernel is executed in a GPU with a total of 96 process blocks, each block corresponding to one individual. Each block is composed by 64 processes, where each process simulates the FBG response at a given wavelength by using the transfer matrix method. Each process performs the necessary matrix multiplications, computing the error between the computed response and the target spectrum. When all processes finish their execution, those errors computed at each wavelength are summed up by using a parallel reduce operator so as to compute the MSE. The kernel creates a total of $96 \times 64 = 6,144$ processes at each iteration, and the number of actual parallel processes is dependent of GPU hardware used. To reduce the global memory usage in the GPU, each process block shares the information about the individual analyzed, with the FBG parameters stored in static read-only global memory. The number of individuals was determined empirically, with the number 96 being favored since it is a multiple of 16, what corresponds to a *warp* or half process block. The proposed methodology allows taking advantage of the available GPU architecture: the resolution can be increased (the number of wavelengths evaluated per individual) in GPUs that accepts a higher number of parallel processes without resulting in a significant performance loss.

D. Experiments

Three experiments ($E1$, $E2$ e $E3$) were performed to evaluate the computational performance of the DE algorithm, and its convergence of the solution to the target deformation profile. Each experiment employed a different target deformation profile, shown in Figure 5. Experiment $E1$ used a linear gradient, while experiment $E2$ used a mirroring of the $E1$ profile, so as to verify the ability of the method to overcome the ambiguity problem mentioned in Section II-A. Experiment

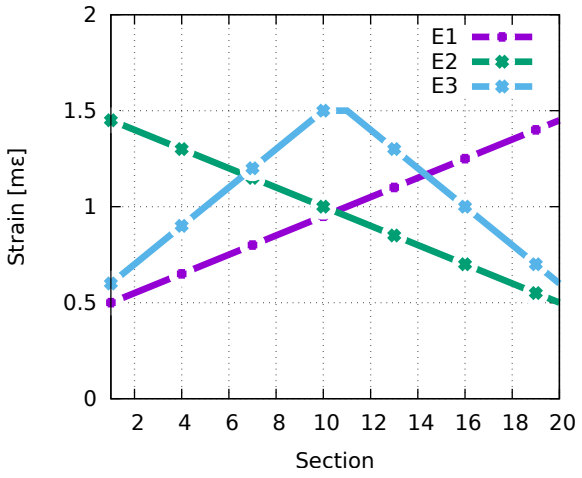

Fig. 5. Deformation profiles employed in experiments $E1$, $E2$ e $E3$. The profile from $E1$ is the mirrored profile from $E2$. The profile for $E3$ is a symmetric trapezoid.

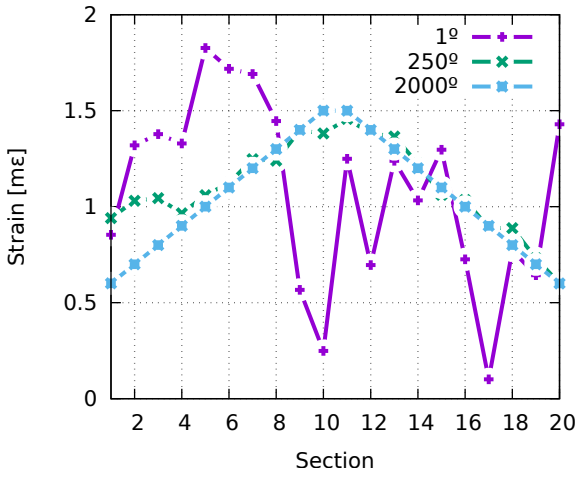

Fig. 6. Example of the evolutionary optimization, showing the evolution of the best individual during the process. This example employed the deformation profile from $E3$ as target.

$E3$ used a trapezoidal deformation profile. All experiments were performed using a NVIDIA GeForce®GTX480 GPU in a desktop with an Intel®Core™2 Quad Processor Q9550 and 8 GBytes of RAM.

During the fitness evaluation, the FBG reflection spectra were simulated with a total of 64 points, distributed in the wavelength range from 1552 nm to 1555 nm, corresponding to the spectral response band of the analyzed FBGs. The parameters employed in the simulations are shown in Table I:

TABLE I. PARAMETERS USED TO SIMULATE THE SPECTRAL RESPONSE OF THE FBGS.

Parameter	Value
p_{11}	0.113
p_{12}	0.252
v_f	0.17
l	1 cm
Λ	532.4 nm
$\overline{n}$	1.457
Δn	2.5×10^{-4}
$\delta\Lambda$	5×10^{-8}
α	5

The mean absolute error (MAE) between the resulting deformation profile and the target deformation profile was used as error metric. Equation 9 was used to compute the MAE, where n_s is the number of segments of the FBG, $target_i$ is the target strain in the i-th segment and $result_i$ is the resulting strain in the i-th segment. Considering that the proposed method is stochastic, each experiment was repeated $1,000$ times to obtain a mean and standard deviation of the results.

$$MAE = \sum_{s=1}^{n_s} |target_i - result_i| \tag{9}$$

III. RESULTS

Figure 6 shows an example of how the best individual evolves during the evolutionary method, having the deformation profile from $E3$ as target.

TABLE II. RESULTS OF $1,000$ REPETITIONS OF EXPERIMENTS $E1$, $E2$ AND $E3$.

Experiment	MAE [mϵ]
$E1$	0.006937 ± 0.078082
$E2$	0.009022 ± 0.050273
$E3$	0.003254 ± 0.040156

A summarization of the experiments is shown in Table II, while the complete results (MAE computed for every repetition of all experiments) are shown in Figure 7. Each repetition took approximately 0.67 s to be executed.

IV. DISCUSSION

As shown in Table II, the mean value of the resulting MAE, for all experiments, is in the order of $\mu\epsilon$. Results from Table II also showed a standard deviation higher than the mean value, stating that some repetitions did not converge to the global optimum. This fact can also be observed by analyzing the results shown in Figure 7, where a relatively small number of repetitions differs in orders of magnitude from the others, also indicating convergence to some local optimum that are distant from the global optimum.

Results shown in Table II and Figure 7 also showed that, for most repetitions, the proposed method converges to solutions close to the target deformation profile. This is achieved without using an additional FBG.

As shown in Section III, the proposed method demands less than 1 second for its execution using a GPU for the evaluation of the fitness. Comparing to the execution time of 10 hours seen in the literature for a method that also does not demand phase information [7], an enhancement of 3 orders of magnitude was achieved. Comparing to the results of a previous implementation of the method (see [10]), it is observed that the GPU implementation can reduce the required computational time by a factor of 19. The new computational cost allows the use of the method in applications that require a response time up to seconds instead of hours, such is the case of online monitoring.

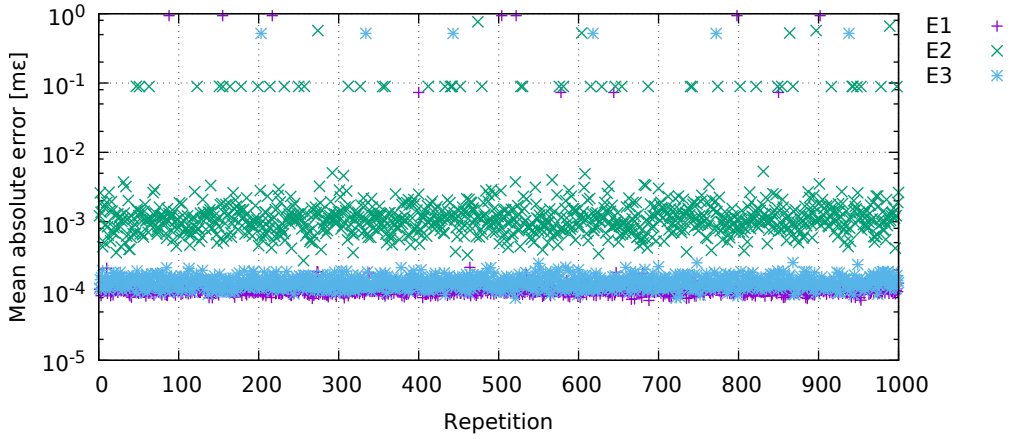

Fig. 7. MAE of each repetition of the experiments.

V. Conclusion

Results showed that the proposed method decreased the computation time in orders of magnitude in respect to the methods previously found in the literature [7], [10]. This improvement was obtained with an efficient implementation of the DE method in GPU. This fact enables the use of the proposed the method to many applications that require reduced processing times. Moreover, the results highlighted the parallelization features of evolutionary optimization methods, showing that it is possible to take advantage of the parallel architecture of GPUs to enhance their computational performance.

Overall, the method is very promising and can be easily adapted for dealing with similar tasks by adjusting the fitness function. Examples of similar tasks include the determination of temperature gradients and its application in the design of FBGs with arbitrary responses.

Acknowledgments

The authors acknowledge the collaboration of Dr. Hugo A. Perlin from the Paraná Federal Institute of Education, Science and Technology - Paranaguá and the financial support received from the CAPES, CNPq, FINEP, and Fundação Araucária Brazilian organizations.

References

[1] A. D. Kersey, M. Davis, H. Patrick, M. LeBlanc, K. Koo, C. Askins, M. Putnam, and E. Friebele, "Fiber grating sensors," *Journal of Lightwave Technology*, vol. 15, no. 8, pp. 1442–1463, 1997.

[2] M. Ohn, S. Huang, R. Measures, and J. Chwang, "Arbitrary strain profile measurement within fibre gratings using interferometric Fourier transform technique," *Electronics Letters*, vol. 33, no. 14, p. 1242, 1997.

[3] M. A. Muriel, J. Azaña, and A. Carballar, "Fiber grating synthesis by use of time-frequency representations," *Optics Letters*, vol. 23, no. 19, pp. 1526–1528, 1998.

[4] J. Azaña, M. A. Muriel, L. R. Chen, and P. W. E. Smith, "Fiber bragg grating period reconstruction using time-frequency signal analysis and application to distributed sensing," *IEEE/OSA Journal of Lightwave Technology*, vol. 19, no. 5, pp. 646–654, 2001.

[5] J. Skaar and R. Feced, "Reconstruction of gratings from noisy reflection data," *Journal of the Optical Society of America. A, Optics, image science, and vision*, vol. 19, no. 11, pp. 2229–2237, 2002.

[6] M. Leblanc, S. Y. Huang, M. Ohn, R. M. Measures, a. Guemes, and a. Othonos, "Distributed strain measurement based on a fiber Bragg grating and its reflection spectrum analysis," *Optics Letters*, vol. 21, no. 17, pp. 1405–1407, 1996.

[7] H.-C. Cheng and Y.-L. Lo, "Arbitrary strain distribution measurement using a genetic algorithm approach and two fiber Bragg grating intensity spectra," *Optics Communications*, vol. 239, no. 4-6, pp. 323–332, 2004.

[8] R. Storn, "On the usage of differential evolution for function optimization," in *Proc. of North American Fuzzy Information Processing Conference*. IEEE, 1996, pp. 519–523.

[9] K. Price, R. M. Storn, and J. A. Lampinen, *Differential Evolution: A Practical Approach to Global Optimization*. Secaucus, NJ, USA: Springer-Verlag, 2005.

[10] L. H. Negri, M. Muller, A. S. Paterno, and J. L. Fabris, "A new approach to solve the inverse scattering problem using a differential evolution algorithm in distributed fiber Bragg grating strain sensors," in *Latin America Optics and Photonics Conference*. Optical Society of America, 2014, p. LTu4A.19.

[11] S. Huang, M. Leblanc, M. M. Ohn, and R. M. Measures, "Bragg intragrating structural sensing," *Applied Optics*, vol. 34, no. 22, pp. 5003–9, 1995.

[12] D. H. Kalegari and H. S. Lopes, "An improved parallel differential evolution approach for protein structure prediction using both 2D and 3D off-lattice models," in *Proc. IEEE Symposium on Differential Evolution (SDE)*, ser. Symposium Series on Computational Intelligence. Piscataway, NJ: IEEE Press, 2013, pp. 143–150.

[13] J. Krause and H. S. Lopes, "A comparison of differential evolution algorithm with binary and continuous encoding for the MKP," in *Proc. of BRICS Congress on Computational Intelligence*. Piscataway, NJ: IEEE Press, 2013, pp. 381–387.